Adsorption of Picric Acid from Aqueous Solution by the Weakly Basic Adsorbent Amberlite IRA-67

Hasan Uslu*,† and Göksel Demir‡

Beykent University, Engineering and Architecture Faculty, Chemical Engineering Department, Ayazağa, İstanbul, Turkey, and Bahçeşehir University, Faculty of Engineering, Department of Environmental Engineering, 34349 Besiktas, İstanbul, Turkey

The presence of nitrophenols in wastewater is of great environmental concern. Therefore, it is important to separate picric acid from wastewater streams. In this study, adsorption of picric acid was studied from aqueous solutions by using a weakly basic adsorbent (Amberlite IRA-67) at three different temperatures (298 K, 308 K, and 318 K). Adsorption of picric acid was investigated in terms of equilibrium, kinetics, and thermodynamic conditions. In the equilibrium studies, 1.00 g of Amberlite IRA-67 was determined as the optimal amount. The most used isotherms, Freundlich and Langmuir, were applied to the experimental data. The Langmuir isotherm gave good results with *R* squared values over 0.99 at different temperatures. In the kinetic studies, pseudofirst- and pseudosecond-order models and the Elovich equation were applied to the kinetic experiments. The pseudosecond-order model was fitted to this adsorption system with an *R* squared value of 0.996. In the thermodynamic studies, $\Delta H^0_{ads} = -21.204$ kJ·mol^{-1}, $\Delta S^0_{ads} = -200.043$ J·mol^{-1}·K^{-1}, and ΔG^0_{ads} for different temperatures were calculated.

1. Introduction

Organic impurities even in low concentrations may be an impediment to the use of water purification techniques. Therefore, a major focus of research has become the removal of these impurities and policy debate in relation to polluted water treatments.[1,2] An environmental problem is the presence of nitrophenols in wastewater streams. Nitrophenols are usually found in effluent wastes from explosive industries, textile industries, and photodegradation of pesticides, and so forth.[3,4] As a consequence of increasing stringent environmental regulations, many methods such as adsorption, chemical oxidation, photodegradation, biological degradation, and solvent extraction have been studied to remove phenolic compounds from industrial wastewater streams.[5−10] Particularly, adsorption methods have been used for the removal of organic compounds from wastewater streams.[11] Activated carbon, as an adsorbent, has been employed many times for the removal of phenolic compounds from wastewater because of its low cost and the ability to regenerate by thermal means.[2,12−15]

Weakly basic ion exchangers are also used for the removal of acids from wastewater streams. Liu and Ren[16] studied the adsorption equilibria of levulinic acid. Uslu[17] reported the removal of formic acid from wastewater streams by adsorption using Amberlite IRA-67, a weak anion exchanger. He reported that Amberlite IRA-67 is an effective adsorbent for the removal of acids from aqueous solutions because of complex formation between acid and amine. Acid (such as picric acid) adsorption on Amberlite IRA-67 is a neutralization reaction shown by the following equation,

$$n(\mathrm{RN}) + \mathrm{AH}_n \leftrightarrow \mathrm{R(NH^+)}_n\mathrm{A}^{n-}$$

where $n = 1$ for picric acid and an acid−amine complex is formed. RN denotes a tertiary amine; [AH] represents picric acid formation in the acid−amine complex ($\mathrm{R(NH^+)}_n\mathrm{A}^{n-}$).

Therefore, the aim of this study was to investigate adsorption efficiency of Amberlite IRA-67 for picric acid from wastewater streams. The thermodynamic parameters, ΔH^0_{ads}, ΔS^0_{ads}, and ΔG^0_{ads}, were calculated. Regeneration was not within the scope of this study.

2. Materials and Methods

2.1. Materials. Picric acid (2,4,6-trinitrophenol) (purity > 97 %) and Amberlite IRA-67 were obtained from Merck Co. Amberlite IRA-67 is a weakly basic gel-type polyacrylic resin with a tertiary amine functional group. It was used without further treatment due to its high purity.

2.2. Equilibrium Methods. Five different concentrations of picric acid were prepared for the equilibrium studies. These concentrations were 4.00 g·L^{-1}, 6.00 g·L^{-1}, 8.00 g·L^{-1}, 10.00 g·L^{-1}, and 14.00 g·L^{-1}. The concentration 14.00 g·L^{-1} is the maximum solubility of picric acid in water at 298 K.

The known amount of adsorbent is presented in Table 1, and a 15 mL picric acid solution was prepared; equilibration studies were carried out in a thermostatic shaker. The period for equilibrium was determined as 90 min. The samples were shaken for 120 min, and the optimum amount of adsorbent was determined as 1.0 g for IRA-67. After equilibration, an aqueous phase sample was titrated to determine the amount of picric acid by NaOH (0.1 N) with phenolphthalein as an indicator. Each experiment was carried out at three different temperatures (298 K, 308 K, and 318 K). Adsorption isotherms were applied according to an optimum amount of IRA-67.

2.3. Kinetic Methods. The kinetic experiments were carried out in a 250 mL stirred cell. The cell was equipped with a

* Corresponding author. E-mail: hasanuslu@gmail.com. Tel.: +90 535 622 07 40.
† Beykent University.
‡ Bahçeşehir University.

10.1021/je100088u
Published on Web 08/06/2010

Table 1. Experimental Results of the Adsorption of Picric Acid onto Amberlite IRA-67 at Different Temperatures (298 K, 318 K, 328 K)

initial conc.		equilibrium conc.	equilibrium conc.	equilibrium conc.	removal of acid	removal of acid	removal of acid
C_o	amount of IRA 67	298 K	318 K	328 K	298 K	318 K	328 K
$g \cdot L^{-1}$	g	C ($g \cdot L^{-1}$)	C ($g \cdot L^{-1}$)	C ($g \cdot L^{-1}$)	(%)	(%)	(%)
4	0.25	1.10	1.21	1.30	72.50	69.75	67.50
4	0.50	0.83	0.95	1.04	79.25	76.25	74.00
4	0.75	0.55	0.69	0.78	86.25	82.75	80.50
4	1.00	0.20	0.29	0.38	95.00	92.75	90.50
4	1.25	0.16	0.26	0.36	96.00	93.50	91.00
6	0.25	1.94	2.08	2.17	67.67	65.33	63.83
6	0.50	1.61	1.70	1.76	73.17	71.67	70.67
6	0.75	1.28	1.35	1.44	78.67	77.50	76.00
6	1.00	0.85	0.97	1.05	85.83	83.83	82.50
6	1.25	0.80	0.93	1.01	86.67	84.50	83.17
8	0.25	2.85	2.96	3.07	64.37	63.00	61.62
8	0.50	2.59	2.67	2.76	67.62	66.62	65.50
8	0.75	2.24	2.38	2.45	72.00	70.25	69.38
8	1.00	1.98	2.07	2.13	75.25	74.12	73.37
8	1.25	1.89	1.99	2.09	76.37	75.12	73.87
10	0.25	3.79	3.90	3.99	62.10	61.00	60.10
10	0.50	3.51	3.65	3.72	64.90	63.50	62.80
10	0.75	3.14	3.29	3.37	68.60	67.10	66.30
10	1.00	2.77	2.91	3.00	72.30	70.90	70.00
10	1.25	2.71	2.87	2.96	72.90	71.30	70.40
14	0.25	5.91	6.02	6.14	57.78	57.00	56.14
14	0.50	5.61	5.72	5.83	59.93	59.14	58.36
14	0.75	5.25	5.36	5.44	62.50	61.71	61.14
14	1.00	4.66	4.75	4.84	66.71	66.07	65.43
14	1.25	4.59	4.68	4.77	67.21	66.57	65.93

fish agitator and was rotated at high speed [(1100 to 1200) rpm] to prevent bulk diffusion as a controlling step of adsorption kinetics as suggested by Azizian et al.[18] The volume of solution was 15 mL, and the amount of IRA 67 was 1.0 g as in the equilibrium experiments. At appropriate time intervals, samples of 1 mL of solution were taken from the vessel and analyzed by a titration method with 0.1 N NaOH and phenolphthalein indicator. The kinetic experiments were carried out at a 14.00 $g \cdot L^{-1}$ concentration of picric acid, which was the maximum solubility of picric acid in water at 298 K; each experiment was repeated twice, but the average values were used.

2.4. FTIR Analysis. Fourier transform infrared (FTIR) analysis has been done with a DIAMOND ATR module of the Nicolette FTIR equipment. Information on the nature of possible interactions between Amberlite IRA-67 and picric acid has been obtained by FTIR spectroscopy. Figure 1 shows the FTIR spectra of Amberlite IRA-67 after (a) and before (b) adsorption. The broad and strong band at 3337 cm^{-1} is due to the overlapping of −OH, aromatic C−H, and NH_2 stretching vibrations. Also, the peak at 1635 cm^{-1} was attributed to the stretching vibration of the amine group N−H. After adsorption, the stretching vibration peaks at 3337 cm^{-1} and 1635 cm^{-1} were shifted to 3295 cm^{-1} and 1630 cm^{-1}, respectively, and the NO_2 groups of picric acid appear at 1560 cm^{-1} as an asymmetric group and 1259 cm^{-1} as a symmetric group. The results indicated that the adsorption could be carried out by ion exchange between Amberlite IRA-67 and picric acid via hydrogen atoms.

3. Results and Discussion

3.1. Equilibrium Studies. In this study, first, the period of the equilibrium state of the adsorbents was determined; the effect of the amount of adsorbent on adsorption was investigated. Second, the effect of initial acid concentration on adsorption was determined. Finally, Langmuir and Freundlich isotherms were applied.

3.1.1. Effect of Amount of Adsorbent. The effect of adsorbent dose on the extent of solute adsorption was investigated by varying dose from (0.25 to 1.25) g IRA-67 for each initial picric acid concentration from 4.00 $g \cdot L^{-1}$ to 14.00 $g \cdot L^{-1}$ at different temperatures of 298 K, 308 K, and 318 K. It was observed from Table 1 that, as the dose increases, the amount of solute adsorbed increases as well for each initial acid concentration, but the percentage removal of acid decreases. The maximum adsorption capacity was reached in 1.25 g of IRA-67, but after 1.00 g of Amberlite IRA-67, the capacitiy of adsorption increased very slowly. Hence, 1.00 g of adsorbent is the optimum amount for this adsorption study.

3.1.2. Effect of Initial Acid Concentration. Different initial picric acid concentrations (4.00 $g \cdot L^{-1}$, 6.00 $g \cdot L^{-1}$, 8.00 $g \cdot L^{-1}$, 10.00 $g \cdot L^{-1}$, and 14.00 $g \cdot L^{-1}$) were studied. It is observed from Table 1 and Figure 2 for increasing initial acid concentration from 4.00 $g \cdot L^{-1}$ to 14.00 $g \cdot L^{-1}$ that the adsorbed acid concentration decreased. The removal efficiency, which is defined as the amount of acid adsorbed from aqueous solution onto the adsorbent, decreased from 96.00 % to 56.93 % with increasing initial concentration of picric acid. This may be explained by the saturation of accessible exchangeable sites of the adsorbent.

3.1.3. Adsorption Isotherms. Langmuir and Freundlich isotherms were studied to find the equilibrium characteristics of adsorption.

The Langmuir equation,[18−20]

$$q_A = \frac{K_A Q_o C_e}{1 + K_A C_e} \quad (1)$$

where q_A and Q_0 denote the adsorbent-phase concentrations of picric acid and saturation capacity, respectively. C_e is the equilibrium concentration of picric acid. K_A is the inverse of the Langmuir constant.

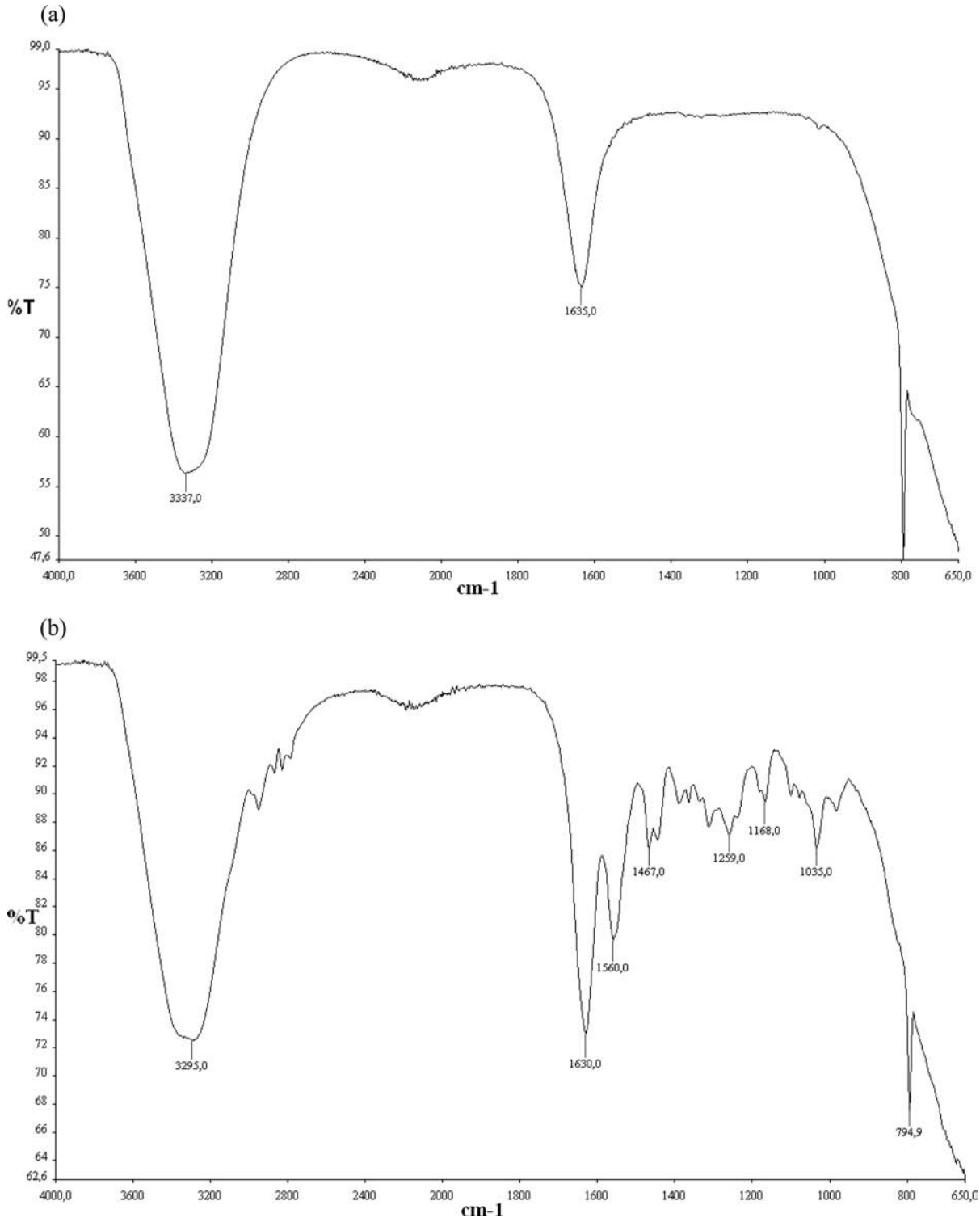

Figure 1. FTIR spectra of Amberlite IRA 67 after (a) and before (b) adsorption.

The values of K_A and Q_o are determined by the following equation into which eq 1 was transformed.

$$C_e = -K_L + C_e\frac{Q_o}{q_A} \qquad K_L = \frac{1}{K_A} \tag{2}$$

The values of K_L and Q_0 are determined from the intercept and slope of the straight line by plotting a graph between C_e and (C_e/q_A). The calculated parameters of the Langmuir equation are presented in Table 2.

The Freundlich isotherm was used in this study as a second isotherm.[21−23]

$$q_A = K_f C_e^{1/n} \tag{3}$$

A logarithmic plot linearizes the equation by enabling the exponent n and the constant K_f to be determined,

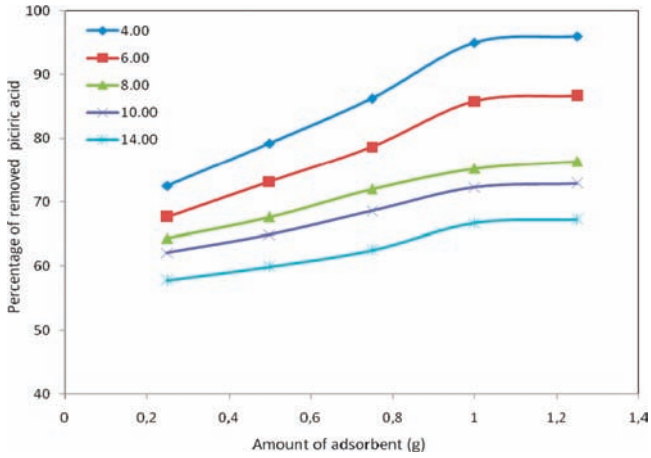

Figure 2. A plot of effect of initial acid concentration on the adsorption of picric acid at 298 K.

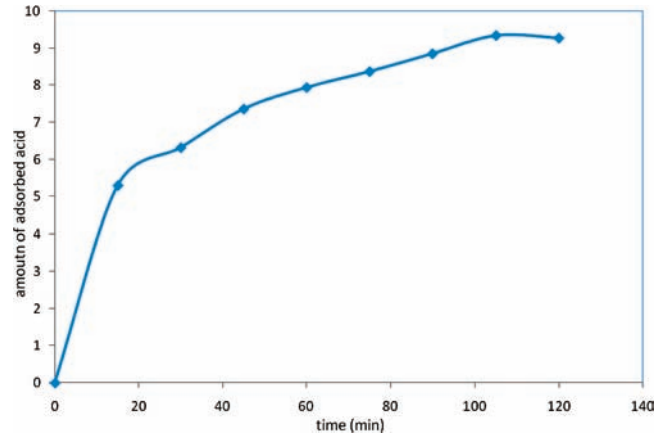

Figure 3. A plot of effect of contact time on the adsorption of picric acid at 298 K.

$$\log q_A = \log K_f + (1/n) \log C_e \quad (4)$$

The values of K_f and $1/n$ at different concentrations were determined from the slope and intercept of the linear plots of log q_A and log C_e. The results of the Freundlich equation are presented in Table 2.

The obtained linear plot with a good correlation coefficient confirms that the Langmuir isotherm is a suitable isotherm for the adsorption of picric acid onto Amberlite IRA-67. The R squared value is over 0.99 for each studied temperature in this study. However, the Freundlich isotherm does not obey the results of adsorption at each temperature. Especially, at 298 K some deviations were observed with the Freundlich isotherm.

3.2. Kinetic Studies. 3.2.1. Effect of Contact Time. The effect of contact time on the adsorption of picric acid by Amberlite IRA-67 was studied for a period of 120 min for initial picric acid concentrations of 14.00 g·L^{-1} at 298 K. The Amberlite IRA-67 dosage was 1.00 g. The effect of contact time on the removal of picric acid is shown in Figure 3 and presented in Table 3. The uptake of adsorbate species is very fast at the initial stages of the contact period, and thereafter, it becomes slower near the equilibrium. In between these two stages of uptake, the rate of adsorption was found to be nearly constant. This is obvious from the fact that a large number of vacant surface sites are available for adsorption during the initial stage. After a lapse of time, the remaining vacant surface sites are difficult to be occupied due to repulsive forces between the solute molecules on the solid and bulk phases.[24]

3.2.2. Adsorption Rate. Various models can be used to analyze the kinetics of sorption processes. Lagergren[25] suggested a rate equation for the sorption of solutes from a liquid solution. This pseudofirst-order rate equation is

$$\frac{dq}{dt} = k_1(q_A - q) \quad (5)$$

Integrating eq 5 with the boundary conditions $t = 0$ to $t = t$ and $q = 0$ to $q = q$ gives the following equation:

$$\ln\left(\frac{q_A - q}{q_A}\right) = -k_1 t \quad (6)$$

where q and q_A are the grams of solute absorbed per gram of sorbent at any time and at equilibrium, respectively, and k_1 is the rate constant of first-order sorption. The pseudofirst-order equation was used extensively to describe the sorption kinetics.[26,27]

If the adsorption kinetics obey a pseudofirst-order model, then a plot of $\ln(q_A - q)$ versus t should be linear. Figure 4 shows a plot for adsorption of picric acid on Amberlite IRA-67. The constants of eq 7 were obtained from Figure 4 at different concentrations and listed in Table 4 with the coefficients of determination, R^2. As is seen clearly from Figure 4 and Table 4, the fitting of the experimental data to the pseudofirst-order model was not so good. Although the coefficients of determi-

Table 3. Effect of Contact Time on the Adsorption of Picric Acid at 298 K

initial conc.	amount of Amberlite IRA-67	equilibrium conc. C_e	removal of acid	time
g·L^{-1}	g	g·L^{-1}	%	min
14.00	1.00	8.70	37.857	15
14.00	1.00	7.68	45.142	30
14.00	1.00	6.64	52.571	45
14.00	1.00	6.06	56.714	60
14.00	1.00	5.63	59.785	90
14.00	1.00	5.15	63.214	105
14.00	1.00	4.66	66.714	120

Table 2. Freundlich and Langmuir Isotherm Parameters of Picric Acid onto Amberlite IRA-67

	Freundlich parameters				Langmuir parameters			
temperature		K_f					K_L	
K	log K_f	mg·mg^{-1}	n	R^2	$1/Q_0$	Q_0	mg·L^{-1}	R^2
298	1.63	42.65	1.48	0.972	0.0314	31.84	0.0428	0.994
308	1.42	26.30	1.39	0.958	0.0259	38.61	0.0315	0.999
318	1.19	15.48	1.23	0.987	0.0212	47.16	0.0250	0.998

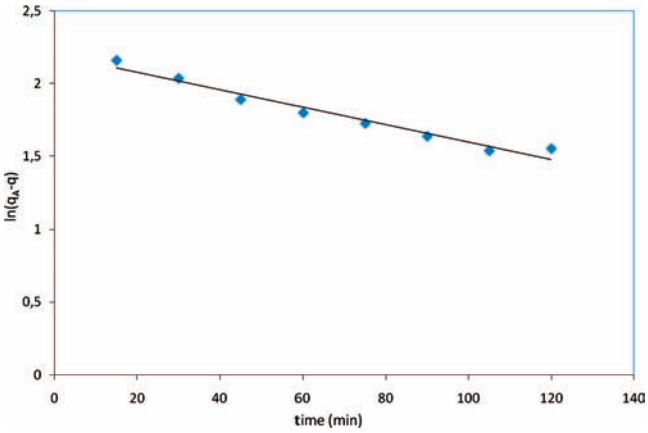

Figure 4. Linear plot of pseudofirst-order kinetic model at 14 g·L^{-1} initial picric acid concentration and 1.00 g of IRA-67.

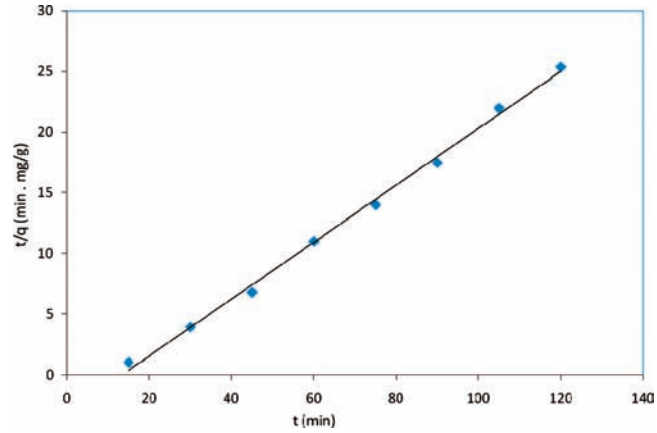

Figure 5. Linear plot of pseudosecond-order kinetic model at 14 g·L^{-1} initial picric acid concentration and 1.00 g of IRA-67.

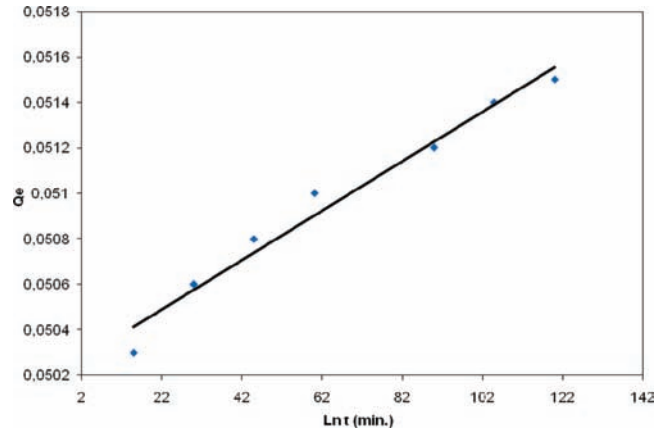

Figure 6. Linear plot of the Elovich model equation.

nation are good, as can be seen in Figure 4, there is a deviation from this model especially at elevated times when t is more than 90 min.

Another model for the analysis of sorption kinetics is the pseudosecond-order model. The rate law for this system is expressed as

$$\frac{dq}{dt} = k_2(q_A - q)^2 \tag{7}$$

Integrating eq 7, for the boundary conditions $t = 0$ to $t = t$ and $q = 0$ to $q = q$, gives

$$\frac{1}{q_A - q} = \frac{1}{q_A} + k_2 t \tag{8}$$

where k_2 is the pseudosecond-order rate constant of sorption. Equation 8 can be rearranged to obtain a linear form,

$$\frac{t}{q} = \frac{1}{k_2 q_A{}^2} + \frac{1}{q_A} t \tag{9}$$

A plot of (t/q) versus t gives a straight line with the slope of $1/(k_2 q_A{}^2)$ and intercept of $1/q_A$. So the gram of solute sorbed per gram of sorbent at equilibrium (q_A) and sorption rate constant (k_2) can be evaluated from the slope and intercept, respectively. The pseudosecond-order model was recently applied to the analysis of sorption kinetics from liquid solutions by Ho and McKay.[28,29]

The values of q_A and k_2 were obtained from the slopes and intercepts of plots in Figure 5. These constants with the coefficients of determination are listed in Table 4. As can be seen in Figure 5, this model fits these experimental results very well.

Table 5. Thermodynamic Parameters for Adsorption of Picric Acid onto Amberlite IRA-67 at Different Temperatures (298 K, 308 K, 318 K)

temperature	ΔG^0_{ads}	K_L	ΔS^0_{ads}	ΔH^0_{ads}
K	kJ·mol^{-1}	mol·L^{-1}	J·mol^{-1}·K^{-1}	kJ·mol^{-1}
298	−20.716	1.868·10^{-7}	−200.043	−21.204
308	−20.626	1.375·10^{-7}		
318	−20.685	1.091·10^{-7}		

3.2.3. Elovich Equation. The Elovich model equation[30] is generally expressed as:

$$\frac{dQ}{dt} = \alpha \exp(-\beta Q) \tag{10}$$

where α is the initial adsorption rate (mg·g^{-1}·min^{-1}) and β is the desorption constant (g·mg^{-1}) during any one experiment. To simplify the Elovich equation, $\alpha\beta t \gg t$ is assumed and by applying the boundary conditions $Q = 0$ at $t = 0$ and $Q = Q$ at $t = t$ equation becomes:

Table 4. Obtained Constant for Pseudofirst-Order and Pseudosecond-Order Kinetic Models at 14 g·L^{-1} Initial Picric Acid Concentration

				pseudofirst-order kinetic model			pseudosecond-order kinetic model		
C_0	Elovich equation			q_A	k_1		q_A	k_2	
g·L^{-1}	α	β	R^2	g·g^{-1}	min^{-1}	R^2	g·g^{-1}	g·g^{-1}·min^{-1}	R^2
14.00	1002	5.18	0.973	1.42·10^{-2}	0.024	0.962	3.46·10^{-2}	35.63	0.996

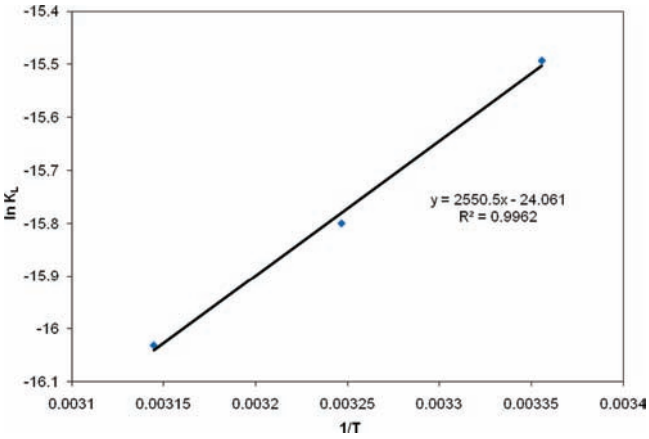

Figure 7. Plot of ln K_L against 1/T.

$$Q = \frac{1}{\beta}\ln(\alpha\beta) + \frac{1}{\beta}\ln(t) \qquad (11)$$

A plot of Q versus ln(t) should yield a linear relationship with a slope of (1/β) and an intercept of (1/β) ln($\alpha\beta$) (Figure 6). The constants are listed in Table 4.

3.3. Thermodynamics Studies. 3.3.1. Effect of Temperature. The effect of temperature on the adsorption of picric acid onto the Amberlite IRA-67 was studied at 298 K, 308 K, and 318 K. Table 1 shows the results of adsorption efficiencies at different temperatures. It can be seen from the experimental results in Table 1 that the adsorption capacity of the IRA 67 is decreasing with increasing temperature.

As related to the temperature effect, the thermodynamic parameters have been calculated for this adsorption system. The free energy change of adsorption ΔG^0_{ads} was calculated by using the equation:

$$\Delta G^0_{ads} = -RT\ln K_L \qquad (12)$$

where R is the universal gas constant and T is the Kelvin temperature. K_L is the thermodynamic equilibrium constant for the adsorption process. It was determined by plotting ln(C_e/q_A) versus C_e and extrapolating to zero C_e as suggested by Khan and Singh.[31]

The other thermodynamic parameters, like the enthalpy change ΔH^0_{ads} and the entropy change ΔS^0_{ads}, were calculated from the slope and intercept of the plots of ln K_L against 1/T according to the following equation:

$$\ln K_L = \frac{\Delta S^0_{ads}}{R} - \frac{\Delta H^0_{ads}}{RT} \qquad (13)$$

ΔH^0_{ads} was obtained from the slope of the straight line and ΔS^0_{ads} was determined from the intercept of the graph.[32,33] To evaluate the thermodynamic equilibrium constant K_L, the C_e/q_A values were plotted versus C_e values at 298 K, 318 K, and 328 K. Linear graphs were obtained for all temperatures. The obtained K_L parameters were used to calculate the ΔG^0_{ads} function.[34] The calculated thermodynamic parameters (ΔH^0_{ads}, ΔS^0_{ads}, and ΔG^0_{ads}) at different temperatures are given in Table 5. ΔH^0_{ads} and ΔS^0_{ads} were obtained from plots of ln K_L versus 1/T as shown in Figure 7.

4. Conclusions

It can be concluded that the use of Amberlite IRA-67 for the adsorption of picric acid is feasible. The use of IRA67 for the adsorption leads to the removal of 96 % picric acid from aqueous solution. The applied isotherms, especially the Langmuir isotherm, showed good results to predict data with an R squared value of over 0.99 at different temperatures. The reaction rate adopted to pseudosecond order. Thermodynamic studies show that this adsorption process is exothermic ($\Delta H^0_{ads} = -21.204$ kJ·mol^{-1}).

Acknowledgment

This work was studied in Beykent University laboratories. We are grateful to Beykent University for supplied chemicals and other equipment. We would like to thank Prof. Dr. Muzaffer Yaşar from Istanbul University for FTIR analysis.

Literature Cited

(1) Senel, S.; Kara, A.; Alsancak, G.; Denizli, A. Removal of Phenol and Chlorophenols from Water with Reusable Dye-Affinity Hollow Fibers. *J. Hazard. Mater.* **2006**, *138*, 317–324.
(2) Dabrowski, A.; Podkoscielny, P.; Hubicki, Z.; Barczak, M. Adsorption of Phenolic Compounds by Activated Carbon, a Critical Review. *Chemosphere* **2005**, *58*, 1049–1070.
(3) Aggarwal, P.; Misra, K.; Kapoor, S. K.; Bhalla, A. K. Effect of Surface Oxygen Complexes of Activated Carbon on the Adsorption of 2,4,6-Trinitrophenol. *Def. Sci. J.* **1998**, *48*, 219–222.
(4) Sepehrian, H.; Fasihi, J.; Mahani, M. K. Adsorption Behavior Studies of Picric Acid on Mesoporous MCM-41. *Ind. Eng. Chem. Res.* **2009**, *48*, 6772–6775.
(5) Banat, F. A.; Al-Bashir, B.; Al-Ashes, S.; Hayajnesh, O. Adsorption of Phenol by Bentonite. *Environ. Pollut.* **2000**, *107*, 391–398.
(6) Dutta, S.; Basu, J. K.; Ghar, R. N. Studies on Adsorption of *p*-Nitrophenol on Charred Saw-Dust. *Sep. Purif. Technol.* **2001**, *21*, 227–235.
(7) Wu, J.; Rudy, K.; Spark, J. Oxidation of Aqueous Phenol by Ozone and Peroxidase. *Adv. Environ. Res.* **2000**, *4*, 339–346.
(8) Hu, X.; Lam, F. L. Y.; Cheung, L. M.; Chania, K. F.; Zhao, X. S.; Lu, G. Q. Copper/MCM-41 as Catalyst for Photochemically Enhanced Oxidation of Phenol by Hydrogen Peroxide. *Catal. Today* **2001**, *68*, 129–133.
(9) Wu, C.; Lui, X.; Wei, D.; Fan, I.; Wang, L. Photosonochemical Degradation of Phenol in Water. *Water Res.* **2001**, *35*, 3927–3933.
(10) Han, W.; Zhu, W.; Zhang, P.; Zhang, Y.; Li, L. Photocatalytic Degradation of Phenols in Aqueous Solution under Irradiation of 254 and 185 nm UV Light. *Catal. Today* **2004**, *90*, 319–324.
(11) Kamble, S. P.; Mangrulkar, P. A.; Bansiwal, A. K.; Rayalu, S. S. Adsorption of Phenol and o-Chlorophenol on Surface Altered Fly Ash Based Molecular Sieves. *Chem. Eng. J.* **2008**, *138*, 73–83.
(12) Tancredi, N.; Medero, N.; Piriz, F. J.; Plada, C.; Cordero, T. Phenol Adsorption onto Powdered and Granular Activated Carbon, Prepared from Eucalyptus Wood. *J. Colloid Interface Sci.* **2004**, *279*, 357–363.
(13) Mohanty, K.; Jha, M.; Meikap, B. C.; Biswas, M. N. Preparation and Characterization of Activated Carbons from Terminalia Arjuna Nut with Zinc Chloride Activation for the Removal of Phenol from Wastewater. *Ind. Eng. Chem. Res.* **2005**, *44*, 4128–4138.
(14) Namane, A.; Mekarzia, A.; Benrachedi, K.; Belhaneche-Bensemra, N.; Hellal, A. Determination of the Adsorption Capacity of Activated Carbon Made from Coffee Grounds by Chemical Activation with $ZnCl_2$ and H_3PO_4. *J. Hazard. Mater.* **2005**, *119*, 189–194.
(15) Tanthapanichakoon, W.; Ariyadejwanich, P.; Japthong, P.; Nakagawa, K.; Mukai, S. R.; Tamon, H. Adsorption-Desorption Characteristics of Phenol and Reactive Dyes from Aqueous Solution on Mesoporous Activated Carbon Prepared from Waste Tires. *Water Res.* **2005**, *39*, 1347–1353.
(16) Liu, B. J.; Ren, Q. L. Sorption of levulinic acid onto weakly basic anion exchangers: Equilibrium and kinetic studies. *J. Colloid Interface Sci.* **2006**, *294*, 281–287.
(17) Uslu, H. Adsorption equilibria of formic acid by weakly basic adsorbent Amberlite IRA-67: Equilibrium, kinetics, thermodynamic. *Chem. Eng. J.* **2009**, *155*, 320–325.
(18) Azizian, S. Kinetic models of sorption: a theoretical analysis. *J. Colloid Interface Sci.* **2004**, *276*, 47–52.
(19) Azizian, S.; Haerifar, M.; Bashiri, H. Adsorption of methyl violet onto granular activated carbon: Equilibrium, kinetics and modeling. *Chem. Eng. J.* **2009**, *146*, 36–41.

(20) Langmuir, I. Constitution and fundamental properties of solids and liquids. *J. Am. Chem. Soc.* **1916**, *38*, 2221–2295.
(21) Iftikhar, A. R.; Bhatti, H. N.; Hanif, M. A.; Nadeem, R.; Nadeem, R. Kinetic and thermodynamic aspects of Cu(II) and Cr(III) removal from aqueous solutions using rose waste biomass. *J. Hazard. Mater.* **2009**, *161*, 941–947.
(22) Coutrin, N. P.; Altenor, S.; Cossement, D.; Marius, C. J.; Gaspard, S. Comparison of parameters calculated from the BET and Freundlich isotherms obtained by nitrogen adsorption on activated carbons: A new method for calculating the specific surface area. *Microporous Mesoporous Mater.* **2008**, *111*, 517–522.
(23) Freundlich, H. Uber die adsorption in losungen. *Z. Phys. Chem.* **1906**, *57*, 385–470.
(24) Rajoriya, R. K.; Prasad, B.; Mishra, I. M.; Wasewar, K. L. Adsorption of Benzaldehyde on Granular Activated Carbon: Kinetics, Equilibrium, and Thermodynamic. *Chem. Biochem. Eng. Q.* **2007**, *21*, 219–226.
(25) Lagergren, S. Zur theorie der sogenannten adsorption gel.oster stoffe. Kungliga Svenska Vetenskapsakademiens. *Handlingar* **1898**, *24*, 1–39.
(26) Cheung, C. W.; Porter, J. F.; McKay, G. Sorption kinetics for the removal of copper and zinc from effluents using bone char. *Sep. Purif. Technol.* **2000**, *19*, 55–64.
(27) Ajmal, M.; Rao, R. A. K.; Ahmad, R.; Ahmad, J. Adsorption studies on Citrus reticulata (fruit peel of orange): removal and recovery of Ni(II) from electroplating wastewater. *J. Hazard. Mater.* **2000**, *79*, 117–131.
(28) Ho, Y. S.; McKay, G. A two-stage batch sorption optimized design for dye removal to minimize contact time. *Trans. Inst. Chem. Eng.* **1998**, *76*, 313–318.
(29) Ho, Y. S.; McKay, G. Kinetic models for the sorption of dye from aqueous solution by wood. *Trans. Inst. Chem. Eng.* **1998**, *76*, 183–189.
(30) Urano, K.; Tachikawa, H. Process development for removal and recovery of phosphorus from wastewater by a new adsorbent. II. Adsorption rates and breakthrough curves. *Ind. Eng. Chem. Res.* **1991**, *30*, 1897–1899.
(31) Khan, A. A.; Singh, R. P. Adsorption thermodynamics of carbofuran on Sn (IV) arsenosilicate in H^+, Na^+ and Ca^{2+} forms. *Colloids Surf.* **1987**, *24*, 33–42.
(32) Tahir, S.; Rauf, N. Thermodynamic Studies of Ni(II) Adsorption onto Bentonite from Aqueous Solution. *J. Chem. Thermodyn.* **2003**, *35*, 2003–2009.
(33) Gupta, V. K.; Singh, P.; Rahman, N. Adsorption behavior of Hg(II), Pb(II), and Cd(II) from aqueous solution on Duolite C-433: a synthetic resin. *J. Colloid Interface Sci.* **2004**, *275*, 398–402.
(34) Demirbas, A.; Sari, A.; Isildak, Ö. Adsorption thermodynamics of stearic acid onto bentonite. *J. Hazard. Mater.* **2006**, *135*, 226–231.

Received for review January 27, 2010. Accepted July 23, 2010.

JE100088U